LAWRENCE
LIVERMORE
NATIONAL
LABORATORY

LLNL-JRNL-418084

Using dissolved noble gas and isotopic tracers to evaluate the vulnerability of groundwater resources in a small, high elevation catchment to predicted climate changes

M.J. Singleton, J.E. Moran

October 15, 2009

Water Resources Research

Disclaimer

Using dissolved noble gas and isotopic tracers to evaluate the vulnerability of groundwater resources in a small, high elevation catchment to predicted climate changes

Michael J. Singleton[1] and Jean E. Moran[2]

1. Chemical Sciences Division, Physical and Life Sciences Directorate, Lawrence Livermore National Laboratory, 7000 East Ave., L-231, Livermore, CA 94550, singleton20@llnl.gov

2. Department of Earth and Environmental Science, California State University East Bay, 25800 Carlos Bee Blvd. Hayward, CA 94542, jean.moran@csueastbay.edu

Submitted to the Water Resources Research special issue, "Climate Change Effects on Groundwater Resources (CLIMATE2)"

1. Abstract

We use noble gas concentrations and multiple isotopic tracers in groundwater and stream water in a small high elevation catchment to provide a snapshot of temperature, altitude, and physical processes at the time of recharge; and to determine subsurface residence times of different groundwater components. We identify three sources that contribute to groundwater flow: 1) seasonal groundwater recharge with short travel times, 2) water from bedrock aquifers that have elevated radiogenic ^{4}He, and 3) upwelling of deep fluids that have "mantle" helium and hydrothermal carbon isotope signatures. Although a bimodal distribution in apparent groundwater age indicates that groundwater storage times range from less than a year to several decades, water that recharges seasonally is the largest likely contributor to stream baseflow. Under climate change scenarios with earlier snowmelt, the groundwater that moves through the alluvial aquifer seasonally will be depleted earlier, providing less baseflow and possible extreme low flows in the creek during summer and fall. Dissolved noble gas measurements indicate recharge temperatures are 5 to 11 degrees higher than would be expected for direct influx of snowmelt, and that excess air concentrations are lower than would be expected for recharge through bedrock fractures. Instead, recharge likely occurs over diffuse vegetated areas, as indicated by $\delta^{13}C$-DIC values that are consistent with incorporation of CO_2 from soil respiration. Recharge temperatures are close to or slightly higher than mean annual air temperature, and are consistent with recharge during May and June, when snowpack melting occurs.

2. Introduction

Predicted changes in the climate will have profound impacts on water resources and water management. Future climate changes in the western United States are likely to include a decrease in the percentage of precipitation that falls as snow, earlier onset of snow-pack melting, an increase in number of rain on snow events, and changes in humidity, air temperature and soil moisture [*Dettinger and Cayan*, 1995; *Howat and Tulaczyk*, 2005; *Maurer and Duffy*, 2005; *Melack, et al.*, 1997] . Snowmelt is an important component of groundwater recharge in high elevation watersheds of the western United States e.g., [*Earman, et al.*, 2006]. In these watersheds, the predicted climate change impacts on snowmelt will likely alter the amount and timing of groundwater recharge, which may lead to reduced groundwater production, declining water tables, and reduced baseflow to streams.

Groundwater aquifers in alpine and sub-alpine basins play a critical role by storing and releasing snowmelt as baseflow to streams long after seasonal precipitation and the disappearance of the snow pack, and in this manner significantly impact stream flow and water temperature. Furthermore, geochemical hydrograph separations have shown that groundwater may supply a majority of alpine streamflow during peak snowmelt conditions [*Liu, et al.*, 2004]. Mountain-block aquifers can also provide significant recharge to mountain-front and basin-fill aquifers [*Manning and Solomon*, 2003; *Manning and Solomon*, 2005]. Despite being an important part of the water supply system, the recharge mechanisms, storage capacity and residence times of high elevation groundwater aquifers are poorly understood and are not adequately characterized by traditional methods. The net change in recharge to mountain aquifers due to alterations in the timing of snowpack melting is not known in sign or magnitude, making it difficult to predict the response of these hydrological systems to climate change.

Dissolved gases are especially well suited to examining recharge processes and groundwater transport in alpine basins, with their large gradients in altitude and

temperature. Dissolved noble gases provide a snapshot of recharge water temperature and physical processes at the time of recharge. Dissolved inorganic carbon concentration, in combination with carbon isotope compositions, are useful for delineating the location of recharge and mixing of different water sources. When combined with measurements of tritium, helium isotopes provide a means of quantifying apparent groundwater subsurface residence time, or groundwater age, over a time scale relevant to the interaction between shallow groundwater and streamflow.

Manning and Caine [2007] used dissolved gas analyses to characterize groundwater recharge and residence times in a high elevation (3300-3900m asl) alpine watershed in Colorado. They determined that permeability decreases with depth and that aquifer parameters are relatively uniform throughout much of the watershed, with mean residence times between 8 and 11 years. Plummer et al., [2001] use dissolved gases to examine groundwater residence in a mountainous region in Shenandoah National Park, Virginia. They found the shallow groundwater system to be dominated by young (<3 yr) water and observed seasonally-varying recharge temperatures, indicating shallow, seasonal recharge. In a study over a much larger geographic area, [*Manning and Solomon*, 2005] used dissolved noble gas results to examine mountain block recharge and subsurface flow to an adjacent basin. Rademacher et al., [2001] found that the apparent groundwater ages of springs in the Sagehen Basin, a small catchment approximately 27 km north of our study site, ranged from 1 to 36 years, and based on the chemical evolution of spring and creek waters, inferred that baseflow to the local creek was dominated by moderately old groundwater [*Rademacher, et al.*, 2005]. Also in the Sagehen Basin, Blumhagen and Clark [2008] used carbon isotope compositions to show that dissolved inorganic carbon in spring waters was inherited from respiration of CO_2 in the soil zone. In this paper, the power of dissolved gas data to evaluate the vulnerability of water resources in high elevation, snow-dominated watersheds, is demonstrated in a small basin likely to experience altered runoff and recharge under warmer climate scenarios. Specifically, the questions that are addressed

using dissolved gas and isotopic analyses are: What are the elevation, temperature, and time period over which recharge takes place? Does water infiltrate through a soil layer/unsaturated zone or through fractures? What is the range in saturated zone residence time for the bulk of the groundwater and for the groundwater most likely to contribute to stream baseflow? One of the challenges in mountain hydrology is access to adequate groundwater sampling points. The research reported here takes advantage of the numerous monitoring wells and production wells in the Olympic Valley groundwater basin.

3. Study Site

The Olympic Valley catchment is located 150 km east of Sacramento, California, near Lake Tahoe in the Sierra Nevada, and has an area of approximately 22 km^2 including alpine and subalpine zones. An alluvial aquifer extends eastward 4 km from the base of Granite Chief, a 2750 m peak that forms the center of Squaw Valley ski area, to the northward-flowing Truckee River (Figure 1). The valley is drained by Squaw Creek, which is formed at the confluence of two major tributaries at the west margin of the basin at elevation 1950 m, entering the Truckee River at 1850 m. The groundwater basin is underlain by Cretaceous granites of the Sierra Nevada batholith, Jurassic metasediments, and Pliocene volcanics that also form the surrounding peaks. Glacial, lacustrine, and fluvial sediments fill the valley to a maximum thickness of 55 m near the center of the 0.8 km wide valley [*Gasch&Associates*, 1973]. A terminal moraine at the eastern end of the basin acted as a sediment dam throughout the Quaternary period.

The hydrogeology of the valley has been examined through drill core logs and surface exposures [*Hydrometrics-LLC*, 2007; *Kleinfelder&Associates*, 1987; *West-Yost&Associates*, 2005] The unconsolidated valley-fill sediments act as an unconfined aquifer except where laterally discontinuous fine grained lacustrine deposits create semi-confined conditions. Three hydrostratigraphic units are loosely defined: a shallow unit consisting of fine grained lake sediments and stream deposits, a middle unit of glacial sands and gravels, and a deep unit comprising fine

grained glacial lake sediments. Coarse-grained materials predominate in the western, upstream portion of the basin and are highly permeable. Sediments become less permeable in the downstream portion of the basin, and at the terminal moraine groundwater occurrence is minimal. Groundwater also occurs in the crystalline rocks, with fractures providing secondary permeability. Four faults are mapped across the valley [*NBMG*, 2000], one of which is coincident with a spring ("Upwelling" spring) near monitoring wells 304/305.

Precipitation in Olympic Valley occurs mainly in the form of snow in the winter months, with a smaller amount of precipitation occurring as rain during spring and summer. A US Department of Agriculture SNOTEL site (site # 784) located at 2447 m elevation in the catchment recorded an average annual precipitation of 1684 mm for the 1982 to 2008 water years (http://www.wcc.nrcs.usda.gov/snotel/). Estimated isohyetals [*Di Luzio, et al.*, 2008] show mean annual precipitation increasing from 1016 mm in the east to 1650 mm in higher elevations to the west. Olympic Valley is uniquely suited to a study of alpine and sub-alpine groundwater because of its relatively simple geometry and because many wells are available for sampling. However, the natural hydrologic cycle is altered through groundwater pumping and possibly because of channelization of the Squaw Creek streambed. Groundwater is extracted to supply the needs of valley residents and businesses (approx. 6.2×10^5 m^3/yr), additional resorts, private residences and the ski area (extraction unknown), snow-making (8.5×10^4 m^3/yr), and for irrigation of a golf course that fills a portion of the meadow surrounding Squaw Creek (2.5×10^5 m^3/yr) [*Hydrometrics-LLC*, 2007]. Peak water demand occurs from July to October and is about twice the wintertime demand. The main production wells are located in a cluster in the western portion of the basin (Figure 1). Although the total groundwater discharge due to pumping is a small fraction of the annual precipitation that falls in the watershed (<4%), the cluster of production wells in the upstream portion of the alluvium does capture water that would contribute to down-gradient flow or to baseflow in Squaw Creek. Fifteen monitoring well pairs are located on and around a golf course in the meadow that covers the lower valley.

A small number of horizontal wells drilled into bedrock produce water at about 0.1 L/min, which is about 10% of the flow rate of the production wells in valley alluvium.

Interaction between the groundwater production wells and stream flow is of concern because of the potential for adversely affecting habitat of brown trout and other fauna. Stream gauging upstream and downstream of the main pumping area indicates that the creek is gaining throughout the annual period of substantial stream flow (November-June). During the summer months, when stream flow decreases to <0.05 m^3/s, the groundwater elevation recorded in production wells adjacent to the stream falls below the elevation of the creek bed (http://www.svpsd.org/scada/aquiferwebdata.html). During the year in which the study was carried out, the upper reach of the creek became dry by late summer, but deep pools and low flow persisted in the lower reach.

4. Methods

This study includes results from eight production wells, including two horizontal wells located about 100 m above the valley floor, 22 monitoring wells, and five stream sampling sites (Figure 1). Samples for DIC were passed through a 0.45 um filter and stored in 40 mL dark glass vials with no headspace. The DIC samples were kept cold in the field and stored in a refrigerator until analysis. Tritium samples were collected in 1 L glass containers with plastic caps. Dissolved gas samples were collected using clear Tygon tubing to connect the sample vessel (8 mm inner diameter copper tubing, 250 mm long) to the wellhead of operating production wells or monitoring wells pumped by a Grundfos submersible pump. Water flowed for several minutes to purge air bubbles. The copper tubing was tapped lightly to dislodge bubbles and a visual inspection for bubbles was made. Steel clamps pinched the copper tubing flat in two locations to secure the water sample.

All analyses were performed at Lawrence Livermore National Laboratory (LLNL). Dissolved inorganic carbon (DIC) and its carbon isotope composition were determined

using the automated DIC-DOC-IRMS technique [*St-Jean*, 2003] consisting of an OI Analytical Model 1030 Carbon analyzer and a Micromass (now Isoprime Ltd) IsoPrime isotope ratio mass spectrometer. Carbon isotope compositions ($^{13}C/^{12}C$) are reported as delta values in per mil relative to the Vienna Peedee Belemnite (VPDB) reference, with an analytical uncertainty of ± 0.3‰. Copper tube samples were mounted on a multi-port gas handling manifold under vacuum. Reactive gases were removed with multiple reactive metal getters. Known quantities of isotopically enriched ^{22}Ne, ^{86}Kr and ^{136}Xe were added to provide internal standards. The isotope dilution protocol used for measuring noble gas concentrations is insensitive to potential isotopic composition variation in dissolved gases (especially Ne) due to diffusive gas exchange. Noble gases were separated from one another using cryogenic adsorption. Helium was analyzed using a VG-5400 noble gas mass spectrometer. Other noble gas isotopic compositions were measured using a quadrupole mass spectrometer. The Ar abundance was determined by measuring the total noble gas sample pressure using a high-sensitivity capacitive manometer. The procedure was calibrated using water samples equilibrated with the atmosphere at a known temperature and air standards spiked with known quantities of the noble gases. Tritium concentrations were determined on 500 g sub-samples by the ^{3}He in-growth method (approximately 25 day accumulation time). Analytical uncertainties are approximately 1% for $^{3}He/^{4}He$, 2% for He, Ne, and Ar, and 3% for Kr and Xe. A detailed description of the data reduction routine is reported in Ekwurzel [2004].

5. Results and Discussion

A total of 34 samples from 25 wells were analyzed for noble gas, and 46 samples from wells and surface water were analyzed for tritium (Table 1). Samples were collected between April and September of 2008. A total of 60 DIC samples were collected from 30 wells, one spring, and 5 stream sampling sites (Table 1).

5.1. Excess Air

The concentration of dissolved noble gases in groundwater is virtually always greater than equilibrium solubility. The portion of gas in excess of equilibrium solubility is termed 'excess air' because of its compositional similarity to air

[*Aeschbach-Hertig, et al.*, 2000; *Holocher, et al.*, 2002]. During transport through the unsaturated zone, infiltrating water may entrain or trap air bubbles that subsequently dissolve in groundwater. Air bubbles may also become trapped in groundwater during fluctuations in the water table. The concentration of excess air provides unique information about the recharge process, including the degree to which infiltrating water incorporates unsaturated zone gas. For dissolved noble gases, addition of excess air has the greatest relative impact on He and Ne concentrations because the equilibrium components of these gases are relatively small.

A common way to represent the amount of excess air is as percent excess Ne, or ΔNe (excess Ne relative to equilibrium component; Table 2). Neon concentrations are used in determining excess air because Ne can be assumed to derive solely from the atmosphere and because Ne is measured with high precision. Excess air may be fractionated during the recharge process and Aeschbach-Hertig, et al. [1999], and later Cey et al.,[2008] examined optimization models to treat fractionated excess air and calculate noble gas recharge temperatures. For samples from Olympic Valley, it was not necessary to use fractionation models because all but two samples (both from MW-PJOW) showed an unfractionated pattern in gas concentrations and a good fit with an unfractionated model of the dissolved noble gas composition. As discussed below, MW-PJOW is located upstream of the other wells in the study area, and unlike the other wells, is recharged mainly from the creek during periods of high flow. The observed fractionation of excess air in MW-PJOW, whereby heavier gases are retained relative to lighter gases (as evidenced by a relatively high ratio of Ne to Xe), is likely the result of relatively large fluctuations in the water table and poor gas confinement.

Recently, Cey et al. [2008] interpreted over 900 analyses of excess air in groundwater samples from the major groundwater basins in California. Results for over 400 samples not affected by artificial recharge (which can greatly increase

240 excess air) are shown in Figure 2, compared with excess air results for 35 samples
241 from Olympic Valley and 31 wells from Handcart Gulch, an alpine watershed in
242 Colorado [*Manning and Caine*, 2007]. Excess air in alpine basins is relatively
243 unexplored, but Manning and Caine [2007] find high excess air concentrations, as
244 shown on Figure 2, associated with bedrock wells, and attribute the high values to
245 large fluctuations in the water table expected for recharge through fractures.
246 Similarly, Plummer et al., [2001] found higher concentrations of excess air in
247 groundwater from wells in fractured rock compared to other wells in Shenandoah
248 National Park. Very low excess air concentrations are expected where an
249 unsaturated zone is not present, as for continuous stream recharge where the water
250 table intersects the surface [*Beyerle, et al.*, 1999; *Kipfer, et al.*, 2002].
251
252 Excess air concentrations in Olympic Valley wells range from ΔNe of 16% to 75%,
253 with an average value of 34% and a median value of 31%, in line with the median
254 value of 28% for the large California data set. These values argue against substantial
255 recharge through fractures. The observed range for Olympic Valley samples
256 suggests that groundwater recharges through an unsaturated zone, but not under
257 conditions of high hydraulic head, large fluctuations in water table height, or very
258 high infiltration rates. Interestingly, this observation holds true for horizontal well
259 samples, which are drilled into fractured bedrock, indicating that recharge through
260 soils overlying the bedrock is likely even at higher elevation in this basin. Average
261 excess air concentrations also argue against stream recharge as the predominant
262 recharge mechanism.
263
264
265 **5.2. Recharge Temperature**
266 Solubilities of the noble gases in fresh water vary as a function of temperature and
267 pressure and are well known from theoretical and empirical studies [*Andrews*,
268 1992] . The strong temperature dependence, especially for the heavy gases, makes
269 it possible to determine the temperature at the water table at the time of recharge
270 [*Stute and Schlosser*, 1999]. Cey et al., [2009] demonstrate that recharge

temperatures determined from noble gas concentrations are very close to measured water table temperatures. Using inverse modeling, the recharge temperature and pressure are determined from noble gas concentrations. However, simultaneous estimation of both temperature and pressure results in a poorly resolved solution because these two parameters are strongly correlated. In general, pressure (or elevation) is more easily constrained by geographic conditions; once an elevation is estimated, temperature is well constrained.

Noble gas recharge temperatures (NGRTs) are calculated from Xe concentrations, after subtraction of the excess air component. Ar and Kr concentrations are used to check the goodness of fit between measured and modeled values, which is reported as X^2 (Table 2). For this sample set, X^2 values are all <11, with 27 out of 35 samples <2, and an average value of 1.5, indicating an acceptable fit for all samples. NGRTs, calculated assuming a recharge elevation of 1950 m, range from 5.3±0.6 to 11.4±0.8 ° C, with an average value of 7.7 ° C. The assumed recharge elevation of 1950 m is close to the break in slope between the surrounding mountainous area and the valley floor, and about 50 m above wellhead elevations, which is a likely elevation of recharge for the basin groundwaters.

Increasing the elevation in the recharge calculations will lead to lower calculated NGRTs. We can therefore calculate a minimum recharge temperature by assuming that the sample was recharged at the very top of the catchment (2750 MASL). Assuming the maximum recharge elevation for the catchment results in a minimum recharge temperature of 3.0±0.6 °C. The highest recharge temperature, assuming maximum elevation, is 8.9±0.7, and the mean of all the samples is lowered to 5.4 °C. It is unlikely that any significant proportion of the groundwaters are recharged at this high elevation given the very small area available. A wider range of recharge elevations that covers much of the surface area, from 2300 m to 1950 m, gives a mean recharge temperature that ranges from 6.7 °C to 7.7 °C. Given that this difference is close to the analytical uncertainty for most measurements, we will use

1950 m as an estimate for elevation when calculating recharge temperatures for most wells. We will use a recharge elevation of 2050 m for the horizontal wells, since they are located approximately 100 m above the valley floor.

Even the minimum possible recharge temperatures calculated for the Olympic Valley wells are significantly higher than the melting point of snow and ice. If we assume that most recharge originates as snowmelt, then the water temperature must have increased prior to reaching the water table. This observation would indicate that an unsaturated zone is present during recharge rather than a direct connection between groundwater and the land surface, and that the infiltrating water has a residence time that allows for equilibration with the soil gas temperature.

In general, soil temperatures near the surface show a damped version of surface temperature variations, but deeper in the unsaturated zone, temperatures approach the mean annual air temperature (MAAT) e.g., [*Cey, et al.*, 2009; *Kipfer, et al.*, 2002]. Flint et al. [2008] measured soil temperatures at a site near Yosemite at a similar elevation (2130 masl) to the Olympic Valley, and found that soil temperatures were fairly stable and increased with depth between 10 and 72 cm under a melting snowpack. Once the snowpack disappeared, Flint et al. [2008] observed a rapid increase in soil temperatures.

The recharge temperatures calculated for Olympic Valley wells fall close to or slightly above the long-term MAATs reported for the nearby Tahoe City NASA GISS Climate Station (http://data.giss.nasa.gov/gistemp/station_data/), which is located approximately 7 km to the southeast of Olympic Valley at an elevation of 1899 m (Figure 3). In most cases soil gas temperatures are slightly greater (1 to 3°C) than the MAAT, so it is common for NGRTs to be slightly greater than MAAT [*Kipfer, et al.*, 2002]. Groundwaters with recharge temperatures more than 2°C above the MAAT may have recharged during warmer months, after most of the snowpack had melted. The average maximum recharge temperature for groundwater samples (7.7 °C) falls

very close to the long-term average air temperature for May (7.8 °C), when there is significant snowmelt (Figure 3C). The higher recharge temperatures fall closer to the long-term mean air temperature in June (11.4 °C). This overlap between recharge temperatures and monthly mean air temperatures suggests that most recharge takes place over a 2-3 month period during the snowmelt season. There is no discernable trend toward higher or lower recharge temperature values with apparent age [Figure 3B]. However, the large range in NGRTs observed in samples with mean apparent ages ≤1 year (discussed in the next section) likely shows the effects of seasonal recharge, with lower temperatures reflecting recharge at the beginning of the melting period and higher temperatures reflecting late season recharge. In wells producing water of mixed age, NGRTs represent mean, integrated values for the mixtures.

5.3. Tritium concentrations and Groundwater ages

All but two of the samples have tritium (^{3}H; half life 12.32 yr) concentrations above the detection limit of 1 pCi/L (Table 1), signaling the presence of groundwater recharged within the last 50 years. Most of the tritium concentrations overlap with the expected range for modern day precipitation, which limits the utility of tritium concentrations alone for determining ages. This range also overlaps with the tritium concentration measured in Squaw Creek, which ranged from 9.7 pCi/L in September, 2008 to 12.4 pCi/L in April, 2008, with a mean for six measurements of 11.1 pCi/L (Table 1). Well values at the high end of the observed range are the result of a contribution from global fallout from nuclear testing, while observed low values are the result of decay, or dilution with older, tritium-free water.

Mean apparent groundwater ages, calculated from tritium and tritiogenic ^{3}He concentrations, are shown in Table 2. In order to determine tritiogenic ^{3}He, the measured ^{3}He and ^{4}He must be adjusted for contributions from the atmosphere (equilibrium solubility and excess air) and from subsurface sources [*Cook and Solomon*, 1997; *Ekwurzel, et al.*, 1994; *Schlosser, et al.*, 1988; *Schlosser, et al.*, 1989]. A significant buildup of radiogenic ^{4}He due to decay of U and Th in crustal rocks

363 takes place as the saturated zone residence time increases [*Andrews, et al.*, 1985;
364 *Torgersen and Clarke*, 1985]. Radiogenic ^{4}He is the portion of measured ^{4}He
365 remaining after subtracting solubility and excess air components. In addition,
366 magmatic fluids can contribute dissolved helium that has a much higher $^{3}He/^{4}He$
367 ratio than atmospheric or crustal sources. The observed tritium and dissolved
368 helium compositions indicate that all of these components must be considered in
369 the analysis of Olympic Valley groundwater.
370
371 In examining samples with a mixture of ages, it is useful to determine the fraction of
372 the mixture that recharged before about 1950 (the time of large increases in global
373 atmospheric ^{3}H due to nuclear weapons testing). The reported tritium-helium age is
374 the mean apparent age of the portion of the sample that contains tritium above the
375 detection limit. A rough estimate of the 'percent pre-modern' is determined by
376 comparing the initial ^{3}H in a sample (i.e., measured $^{3}H + {}^{3}He_{tritiogenic}$) with the ^{3}H in
377 precipitation at the time and location of recharge (Figure 4). The nearest IAEA GNIP
378 stations where ^{3}H in precipitation data were collected are Santa Maria, CA, and
379 Menlo Park, CA (http://www-naweb.iaea.org/napc/ih/GNIP/IHS_GNIP.html), but
380 these are incomplete records in very different physiographic settings than Olympic
381 Valley. Figure 4 shows an exponential fit to mean annual averaged data for Western
382 North America, along with measured values from two cities with long records.
383 Several points for groundwater samples from Olympic Valley with apparent ages
384 older than 10 years fall below the curve. If one assumes 'piston flow' of
385 groundwater, without mixing of post-modern groundwater during transport, the
386 percentage of pre-modern water is calculated according to the difference between
387 the expected value on the curve, and the observed value below the curve. For
388 exponential mixing of post-modern water [*Cook and Böhlke*, 1999], the initial ^{3}H
389 curve is generally somewhat lower than the smoothed curve, so smaller pre-modern
390 percentages would be calculated. In any case, samples with the oldest tritium-
391 helium ages are mixed with a significant component of pre-modern water.
392
393 Olympic Valley groundwater samples fall into three groupings: 1)samples with very

young mean apparent ages and little pre-modern water, 2)samples with a component of relatively young, tritiated water mixed with older, pre-modern water containing radiogenic ^{4}He, and 3)samples with a smaller component of young water, mixed with older water and magmatic fluids.

The three groups are distinguishable on a plot of ^{3}He/^{4}He versus Ne/He (Figure 5). On this plot, Ne and He concentrations are adjusted by subtracting the excess air component of each. For comparison, values for air saturated water at 8°C are also shown. Ne has only an atmospheric source, while He may be affected by the build-up of crustal He, accumulation of tritiogenic ^{3}He, or addition of magmatic He. Crustal He can contribute both ^{3}He (via an α,n reaction on ^{6}Li) and ^{4}He (via α decay of natural U and Th); the effect is insignificant for ^{3}He but can be very large for ^{4}He, so an increase in crustal He results in a decrease in Ne/He. Magmatic He sources have high ^{3}He/^{4}He and typically high He concentrations. On Figure 5, samples with magmatic He stand out as having high ^{3}He/^{4}He and low Ne/He, while samples with a component of radiogenic ^{4}He have Ne/He ratios lower than air saturated water (corresponding to wells with radiogenic ^{4}He concentrations >$2x10^{-9}$ cm^3STP/gH_2O in Table 2). Addition of tritiogenic ^{3}He due to decay of ^{3}H causes an increase in ^{3}He/^{4}He above values expected for atmospheric sources of He.

5.3.1. Recent recharge

In the first group are two monitoring wells and four production wells that yield water with a mean apparent age of less than 1 year (with a 2 sigma analytical uncertainty of about 1 year) and no detectable pre-modern water. Groundwater ages of 1 year or less in long screened, high flow wells are unusual; fewer than 2% of drinking water wells examined under California's Groundwater Ambient Monitoring and Assessment (GAMA) program (http://www.swrcb.ca.gov/gama/) (n=1317) have apparent tritium-helium ages ≤1 year. The wells producing very recent recharge are located in the western portion of the basin where coarse-grained

glacial and fluvial sediments prevail, which likely exhibit high hydraulic conductivity. This vigorous flow system is recharged on a short time scale (one year or less) and over a limited spatial extent (given the short time period for saturated zone transport). The production wells in this group, with screened intervals from 11 to 20 m long, do not reach depths near the bedrock basement (Figure 6). Although the creek is not likely a major source of recharge to these wells (as discussed below), the predominance of young groundwater in the alluvial aquifer suggests that it is this young component that likely provides much of the baseflow to the stream. Under climate change scenarios with earlier snowmelt and runoff, this groundwater reservoir will be depleted earlier, providing less baseflow and possible extreme low flows in the creek during summer and fall.

Several of the lower valley monitoring wells and the two horizontal wells (Figure 7) exhibit somewhat older ^{3}H-^{3}He apparent ages. The apparent groundwater ages calculated for these wells give the groundwater age histogram its bimodal character (Figure 7). These wells are grouped with wells dominated by relatively recent recharge because they do not share dissolved gas characteristics associated with bedrock groundwater. The wells do not produce groundwater containing radiogenic ^{4}He, they just have higher concentrations of tritiogenic ^{3}He than samples with <1 year ages (Figure 5). In contrast to the production wells with <1 year mean ages, many of these wells are screened in lower permeability media, which includes near surface fine grained sediments in the lower valley and near surface fractured rock (in the case of the two horizontal wells). This older component may contribute to stream baseflow in the lower reaches of Squaw Creek, given its occurrence in shallow monitoring wells adjacent to the creek. Significant flow and deep pools are observed in downstream reaches of the creek later in the water year than in upstream reaches.

5.3.2. Bedrock aquifer flow paths

The remaining production wells (SVPSD Well 1, SVPSD Well 2), well T4, MW 5D, and five of the valley monitoring wells, fall into the second group, drawing a component

of significantly older groundwater as evidenced by a concentration of radiogenic ^4He greater than $2x10^{-9}$ cm^3STP/g and high pre-modern fractions (Table 2). These wells produce mixed aged water, as they also all contain tritium and have mean apparent groundwater ages (for the portion of the water containing tritium) of less than 50 years. All of these wells tap the deeper flow system associated with bedrock that underlies the alluvial fill, either being partially screened in bedrock or being situated near a major fault (Figure 6).

Granitic rocks have comparatively high U and Th concentrations, which can result in a relatively high radiogenic ^4He production rate [*Andrews, et al.*, 1989]. In addition, glacial tills and weathered granites have been shown to exhibit high ^4He release rates into circulating groundwater [*Beyerle, et al.*, 1999; *Van der Hoven, et al.*, 2005]. Nonetheless, radiogenic ^4He concentrations in affected Olympic Valley wells are low in comparison to production wells affected by crustal He in bedrock wells elsewhere [*Holocher, et al.*, 2001; *Manning and Caine*, 2007] and in deep supply wells elsewhere in California [*Van der Hoven and Moran*, in review]. Since this component is not observed in many of the production and monitoring wells screened exclusively in alluvium, the crustal fluid is not likely being produced within the alluvium but may be related to diffusion of ^4He from low permeability bedrock at the base of the alluvial aquifer. Although present at depth, and clearly affecting wells that directly tap bedrock groundwater or are affected by focused flow along faults (Figure 6), this component is minor in comparison to the very young groundwater component, and is not likely to play a significant role in stream interaction or baseflow to the stream.

5.3.3. Upwelling magmatic fluids

Samples that fall into group three have smaller components of recent recharge, along with an older component containing crustal He, and a component of magmatic fluid. Recently, Kulongoski et al. [2005] and Saar [2005] have presented methods for quantifying mixing proportions for groundwaters that have crustal, magmatic, and tritiogenic components, as revealed by examination of the isotopic composition

of dissolved helium. Compared to samples from those studies, Olympic Valley groundwater samples have much smaller magmatic and crustal components. Olympic Valley samples are dominated by atmospheric (equilibrium solubility and excess air) and tritiogenic ^{3}He components. However, because the magmatic $^{3}He/^{4}He$ ratio is drastically different from the $^{3}He/^{4}He$ ratio for other helium sources, the presence of a small component of magmatic fluid in four of the samples makes determination of a ^{3}H-^{3}He age highly unconstrained (age labeled as "^{3}He excess" in Table 2). These samples lie along a transect that lines up with an active fault, Valley Fault 3 (Figure 1 and Figure 6), and are clearly affected by fluid that emanates from a deep, magmatic source. One of these samples, MW 329, contains less than 1 pCi/L ^{3}H and thus is a mixture of only magmatic and crustal components. A simple linear mixing calculation for this sample (using $^{3}He/^{4}He_{magmatic} = 1.22x10^{-5}$; [*Graham*, 2002] and $^{3}He/^{4}He_{crustal} = 6x10^{-7}$ [*Van der Hoven and Moran*, in review]) results in estimates for the magmatic component of only 7%. The other three wells along Valley Fault 3 contain tritium, and tritiogenic ^{3}He, and are complex mixtures of relatively recent recharge, older water with a significant radiogenic ^{4}He component, and magmatic fluid that reaches shallow groundwater via the active fault. One additional monitoring well sample from the lower valley (MW302) may likewise be affected by magmatic He.

5.4. Dissolved Inorganic Carbon

Water samples from the horizontal and production wells contained 16 to 32 mg/L C as DIC with $\delta^{13}C$-DIC values that ranged from -19.1 to -16.4 ‰. The lower valley monitoring wells have $\delta^{13}C$-DIC values that range from -20.9 to 4.2 ‰, with concentrations from 20 to 222 mg/L C. Stream waters are low in DIC concentration (3-13 mg/L C), and have $\delta^{13}C$ values that range from -11.0 to -2.6 ‰.

The carbon isotope values for the production well groundwater samples ($\delta^{13}C$-DIC of -19.1 to -16.4 ‰) are consistent with the incorporation of soil CO_2 during recharge e.g., [*Blumhagen and Clark*, 2008; *Cerling, et al.*, 1991], which reflects a mix

of respiration CO_2 and atmospheric CO_2 sources. The incorporation of soil CO_2 in the production well groundwater suggests that recharge occurs in subalpine areas with developed soils such as the vegetated slopes surrounding the valley, as opposed to the bare rock exposures that form some of the highest elevation gradients surrounding the valley.

When plotted against 1/[DIC], the δ^{13}C-DIC values indicate mixing between three dominant sources (Figure 8): 1) groundwater recharged through the soil zone, 2) recharge from Squaw Creek, and 3) upwelling of magmatic fluids. The compositions of these end members are discussed below.

5.4.1. Recharge through the soil zone

The concentration and isotopic composition of soil CO_2 vary in relation to the respiration rate [*Cerling, et al.*, 1991]. Consequently, recharge through soils with a range of soil respiration rates might be expected to result in a range of DIC concentrations and isotopic compositions. For this reason we selected two potential end members for groundwaters recharged through the soil zone. In both cases, wells with moderate groundwater ages (11 to 16 years) were selected to avoid wells that might receive significant recharge from the creek. The average values of [DIC] (29 mg/L C) and δ^{13}C-DIC (-17.5 ‰) for the Horizontal Wells were selected as the first groundwater end member. The Horizontal wells likely see recharge through soils at higher elevations than the valley monitoring wells. Monitoring well MW-5D was selected as the second groundwater end member, and has an average [DIC] of 17.2 mg/L C and an average δ^{13}C-DIC value of -19.1 ‰.

5.4.2. Squaw Creek Water

The concentrations and isotopic compositions of DIC in the stream water samples are generally consistent with DIC derived from equilibration with atmospheric CO_2, which has a δ^{13}C value of approximately -8 ‰. Some of the stream δ^{13}C-DIC values are slightly higher than the δ^{13}C value of air, suggesting that perhaps some of the

stream DIC is derived from mineral weathering. An end member for Squaw Creek was defined by the average value of samples collected at the lower ends of the southern and northern tributaries to Squaw Creek, above the confluence (Sites 1 and 2 in Figure 1), which have an average [DIC] of 4.6 mg/L C, and an average δ^{13}C-DIC value of -4.8 ‰.

The downstream sampling sites tend to have lower δ^{13}C-DIC values and higher concentrations than the upper parts of the creek, which likely indicates an influx of groundwater along the stream channel (also indicated by stream gauge observations, as noted above). For the purposes of this study, the stream will be considered only as a possible recharge source. A more detailed study quantifying the groundwater influx to the stream is ongoing, and will not be discussed further here.

5.4.3. Upwelling magmatic water

The monitoring wells have a much broader range of DIC concentrations and isotopic compositions. Many of the monitoring wells have DIC compositions similar to the production wells. However, wells along Valley Fault #3 have much higher concentrations of DIC (50-222 mg/L C) and appear to be influenced by a carbon source with δ^{13}C values close to -5 ‰. Similar δ^{13}C values and high [DIC] have been linked to upwelling of magmatic fluids and seismic activity along faults around Mammoth Mountain in California [*Sorey, et al.*, 1998]. A contribution of magmatic water is also consistent with the ^{3}He/^{4}He ratios reported here. Well MW-330 was chosen as an end member to represent groundwaters that have interacted with the upwelling magmatic fluids. Well MW-330 was selected because it had the highest [DIC] of 222 mg/L C, and has no detectable tritium (<1 pCi/L).

5.4.4. Recharge from Squaw Creek

Based on the end members defined above, Squaw Creek does not appear to be a dominant source of recharge for most of the wells sampled in this study. The lone

exception is the monitoring well MW-PJOW, which was the uppermost valley well sampled. Based on samples collected in May and August, the [DIC] and δ^{13}C-DIC in MW-PJOW appears to be derived from between 50% and 70% creek water. The low recharge temperatures calculated for MW-PJOW may indicate that the creek recharge occurs during the cold, high flow conditions during snowmelt runoff. As an alternative, well MW-PJOW may receive recharge from the prominent rock escarpment to the west. Recharge through bare rock fractures would have essentially identical [DIC] and δ^{13}C-DIC values to creek water.

In general, the production wells have much higher [DIC] and much lower δ^{13}C-DIC values than Squaw Creek. This contrast between the isotopic composition and concentration of DIC in the production wells and DIC in stream water suggests that these waters have different sources and indicates that Squaw Creek is not a dominant source of recharge to the production wells. However, based on the end members defined above, samples from production wells SVPSD Well # 1, 2, and 3, fall within the range of [DIC] and δ^{13}C-DIC values that potentially indicate between 10% and 30% of produced water is from Squaw Creek. Quantifying such small contributions of the stream water is highly uncertain due to a strong dependence on the defined compositions of end members. Given the older apparent ages of SVPSD Wells 1 and 2, it is unlikely that they receive significant recharge from the creek. As discussed above, the slightly higher δ^{13}C-DIC values may also indicate the presence of water that was recharged over bare rock. Based on the mixing analysis of DIC, the majority of water at the production wells was recharged through a soil zone. This result is in agreement with the interpretation of excess air results and with stream and well hydrograph observations.

6. Summary and Conclusions

Dissolved gas tracers provide a powerful toolset to evaluate the vulnerability of high altitude watersheds to climate change impacts because they address key questions about recharge location and subsurface residence time. The extent to which

607 individual catchments are vulnerable to climate change will depend largely on the
608 specifics of geology, topography, and climate. The dissolved gas toolset used for this
609 study can be applied under a wide range of potential settings, but is especially useful
610 in high elevation areas because of the steep gradients in precipitation and
611 temperature and because active recharge and vigorous flow results in relatively
612 young apparent groundwater ages, dateable by the tritium-helium method.
613
614 Young groundwaters dominate the alluvial aquifer in Olympic Valley, and likely
615 account for most of the potential baseflow to Squaw Creek. These waters have
616 apparent ages of less than one year and are therefore vulnerable to climate changes
617 over short time scales. Mixed age components also need to be considered in studies
618 of alpine and sub-alpine groundwater residence time. In this study, the bedrock
619 aquifer underlying the valley fill contributes an older component that has
620 accumulated radiogenic ^{4}He. In addition, He and C isotopes show the influence of
621 magmatic fluids in shallow groundwater, especially in the area of an active fault.
622 Evaluating the residence times of groundwater in these systems provides an
623 important constraint on the potential responses of stream baseflow to climate
624 change. The major findings with respect to groundwater residence times in Olympic
625 Valley, i.e., that the alluvial aquifer experiences rapid flushing of seasonal recharge,
626 and that significantly older fluids are found at the bedrock interface that underlies
627 the alluvium, are similar to the major findings of Beyerle et al. [1999] in the
628 Lisenthal aquifer of Switzerland and Plummer et al. [2001] in the Blue Ridge
629 Mountains. Similar studies are needed in bigger catchments to determine whether
630 an increase in scale may decrease the dominance of young waters.
631
632 NGRTs constrain the location and timing of recharge and correspond to air
633 temperatures at the time of snowmelt. Recharge occurs mainly through soil zones
634 where the waters incorporate CO_2 from respiration and recharging water is
635 thermally equilibrated within the unsaturated zone. Recharge through fractures
636 and recharge from the creek is less important in this catchment. Long term
637 monitoring of recharge temperatures may provide a means to gauge watershed

response to climate changes such as an earlier onset of snowmelt and changes in mean air temperature.

7. Acknowledgements

The authors wish to gratefully acknowledge assistance with field sampling and sample analysis by Brad Esser, Sarah Roberts, Darren Hillegonds, Mike Sharp, and Carl Gustafson. Well access and logistical support were provided by Squaw Valley Public Services District, Friends of Squaw Creek, The Resort at Squaw Creek, Squaw Valley Mutual Water Company, and Derrik Williams (HydroMetrics LLC). Funding for this work was provided by LLNL Laboratory Directed Research and Development, Climate Initiative. Jean Moran received support from the Joan Sieber research award at California State University, East Bay.

This work was performed under the auspices of the U.S. Department of Energy by Lawrence Livermore National Laboratory under Contract DE-AC52-07NA27344.

8. References

Aeschbach-Hertig, W., F. Peeters, U. Beyerle, and R. Kipfer (1999), Interpretation of dissolved atmospheric noble gases in natural waters, *Water Resources Research*, *35*, 2779-2792

Aeschbach-Hertig, W., F. Peeters, U. Beyerle, and R. Kipfer (2000), Palaeotemperature reconstruction from noble gases in ground water taking into account equilibration with entrapped air, *Nature*, *405*, 1040-1044

Andrews, J. N. (1992), Mechanisms for noble gas dissolution by groundwaters, in *Isotopes of Noble Gases as Tracers in Environmental Studies*, edited, International Atomic Energy Agency, Vienna

Andrews, J. N., N. Hussain, and M. J. Youngman (1989), Atmospheric and radiogenic gases in ground waters from the Stripa granite, *Name: Geochimica et Cosmochimica Acta*

Andrews, J. N., G. B. Wilson, M. J. Youngman, J. E. Goldbrunner, W. G. Darling, P. J. Hooker, L. Eichinger, W. Rauert, and W. Stichler (1985), Radiochemical, hydrochemical and dissolved gas study of groundwaters in the Molasse basin of Upper Austria, *Name: Earth Planet. Sci. Lett*

676 Beyerle, U., W. Aeschbach-Hertig, M. Hofer, D. M. Imboden, H. Baur, and R. Kipfer
677 (1999), Infiltration of river water to a shallow aquifer investigated with 3H/3He,
678 noble gases and CFCs, *Journal of Hydrology*, *220*, 169-185

679 Blumhagen, E. D., and J. F. Clark (2008), Carbon sources and signals through time in
680 an Alpine groundwater Basin, Sagehen California, *Applied Geochemistry*, *23*, 2284-
681 2291

682 Cerling, T. E., D. K. Solomon, J. Quade, and J. R. Bowman (1991), On the isotopic
683 composition of carbon in soil carbon dioxide, *Geochimica et Cosmochimica Acta*, *55*,
684 3403-3405

685 Cey, B. D., G. B. Hudson, J. E. Moran, and B. R. Scanlon (2008), Impact of artificial
686 recharge on dissolved noble gases in groundwater in California, *Environmental*
687 *Science & Technology*, *42*, 1017-1023

688 Cey, B. D., G. B. Hudson, J. E. Moran, and B. R. Scanlon (2009), Evaluation of Noble
689 Gas Recharge Temperatures in a Shallow Unconfined Aquifer, *Ground Water*, *47*,
690 646-659

691 Cook, P. G., and J. K. Böhlke (1999), Determining timescales for groundwater flow
692 and solute transport, in *Environmental tracers in subsurface hydrology*, edited by P.
693 G. Cook and A. L. Herczeg, Kluwer Academic Publ., Boston, MA

694 Cook, P. G., and D. K. Solomon (1997), Recent advances in dating young groundwater
695 - chlorofluorocarbons, H-3/He-3 and Kr-85, *Journal of Hydrology*, *191*, 245-265

696 Dettinger, M. D., and D. R. Cayan (1995), Large-scale atmospheric forcing of recent
697 trends toward early snowmelt runoff in California, *Journal of Climate*, *8*, 606-623

698 Di Luzio, M., G. L. Johnson, C. Daly, J. K. Eischeid, and J. G. Arnold (2008),
699 Constructing Retrospective gridded daily precipitation and temperature datasets for
700 the conterminous United States, *Journal of Applied Meteorology and Climatology*, *47*,
701 475-497

702 Earman, S., A. R. Campbell, F. M. Phillips, and B. D. Newman (2006), Isotopic
703 exchange between snow and atmospheric water vapor: Estimation of the snowmelt
704 component of groundwater recharge in the southwestern United States, *Journal of*
705 *Geophysical Research-Atmospheres*, *111*, D09302

706 Ekwurzel, B. (2004), LLNL Isotope Laboratories Data Manual, UCRL-TM-203316,
707 133 pp, Lawrence Livermore National Laboratory

708 Ekwurzel, B., P. Schlosser, W. M. Smethie, L. N. Plummer, E. Busenberg, R. L. Michel,
709 R. Weppernig, and M. Stute (1994), Dating of shallow groundwater - comparison of
710 the transient tracers H-3/He-3, chlorofluorocarbons, and Kr-85, *Water Resources*
711 *Research*, *30*, 1693-1708

712 Flint, A. L., L. E. Flint, and M. D. Dettinger (2008), Modeling soil moisture processes
713 and recharge under a melting snowpack, *Vadose Zone Journal*, *7*, 350

714 Gasch&Associates (1973), Squaw Valley Geophysical Investigation, 8 pp

715 Graham, D. W. (2002), Noble gas isotope geochemistry of mid-ocean ridge and ocean
716 island basalts: Characterization of mantle source reservoirs, *Reviews in Mineralogy*
717 *and Geochemistry*, *47*, 247

718 Holocher, J., V. Matta, W. Aeschbach-Hertig, U. Beyerle, M. Hofer, R. Peeters, and R.
719 Kipfer (2001), Noble Gas and Major Element Constraints on the Water Dynamics in
720 an Alpine floodplain, *Ground Water*, *39*, 841-852

721 Holocher, J., F. Peeters, W. Aeschbach-Hertig, M. Hofer, M. Brennwald, W. Kinzelbach,
722 and R. Kipfer (2002), Experimental investigations on the formation of excess air in
723 quasi-saturated porous media, *Geochimica et Cosmochimica Acta*, *66*, 4103-4117

724 Howat, I. M., and S. Tulaczyk (2005), Climate sensitivity of spring snowpack in the
725 Sierra Nevada, *J Geophys Res*, *110*, F04021

726 Hydrometrics-LLC (2007), Olympic Valley Groundwater Management Plan, 104 pp,
727 Squaw Valley Public Services District, Placer County, CA

728 Kipfer, R., W. Aeschbach-Hertig, F. Peeters, and M. Stute (2002), Noble gases in lakes
729 and ground waters, *Reviews in Mineralogy and Geochemistry*, *47*, 615

730 Kleinfelder&Associates (1987), Basin Water Quality Investigation, The Resort at
731 Squaw Creek, Squaw Valley, CA

732 Kulongoski, J. T., D. R. Hilton, and J. A. Izbicki (2005), Source and movement of
733 helium in the eastern Morongo groundwater Basin: The influence of regional
734 tectonics on crustal and mantle helium fluxes, *Geochimica et Cosmochimica Acta*, *69*,
735 3857-3872

736 Liu, F., M. W. Williams, and N. Caine (2004), Source waters and flow paths in an
737 alpine catchment, Colorado Front Range, United States, *Water Resources Research*,
738 *40*, W09401

739 Manning, A. H., and J. S. Caine (2007), Groundwater noble gas, age, and temperature
740 signatures in an Alpine watershed: Valuable tools in conceptual model development,
741 *Water Resources Research*, *43*

742 Manning, A. H., and D. K. Solomon (2003), Using noble gases to investigate
743 mountain-front recharge, *Journal of Hydrology*, *275*, 194-207

744 Manning, A. H., and D. K. Solomon (2005), An integrated environmental tracer
745 approach to characterizing groundwater circulation in a mountain block, *Water*
746 *Resources Research*, *41*, W12412

747 Maurer, E. P., and P. B. Duffy (2005), Uncertainty in projections of streamflow
748 changes due to climate change in California, *Geophys Res Lett*, *32*, L03704

749 Melack, J. M., J. Dozier, C. R. Goldman, D. Greenland, A. M. Milner, and R. J. Naiman
750 (1997), Effects of climate change on inland waters of the Pacific Coastal Mountains
751 and Western Great Basin of North America, *Hydrological Processes*, *11*

752 NBMG (2000), Preliminary Map of Pleistocene to Holocene Faults in the Lake Tahoe
753 Basin, California and Nevada, Nevada Bureau of Mines and Geology

754 Plummer, L. N., E. Busenberg, J. K. Bohlke, D. L. Nelms, R. L. Michel, and P. Schlosser
755 (2001), Groundwater residence times in Shenandoah National Park, Blue Ridge
756 Mountains, Virginia, USA: a multi-tracer approach, *Chemical Geology*, *179*, 93-111

757 Rademacher, L. K., J. F. Clark, D. W. Clow, and G. B. Hudson (2005), Old groundwater
758 influence on stream hydrochemistry and catchment response times in a small Sierra
759 Nevada catchment: Sagehen Creek, California, *Water Resources Research*, *41*,
760 W02004

761 Rademacher, L. K., J. F. Clark, G. B. Hudson, D. C. Erman, and N. A. Erman (2001),
762 Chemical evolution of shallow groundwater as recorded by springs, Sagehen basin;
763 Nevada County, California, *Chemical Geology*, *179*, 37-51

764 Saar, M. O., M. C. Castro, C. M. Hall, M. Manga, and T. P. Rose (2005), Quantifying
765 magmatic, crustal, and atmospheric helium contributions to volcanic aquifers using
766 all stable noble gases: Implications for magmatism and groundwater flow, *Geochem.*
767 *Geophys. Geosyst*, *6*

768 Schlosser, P., M. Stute, H. Doerr, C. Sonntag, and K. O. Muennich (1988), Tritium/
769 3He dating of shallow groundwater, *Earth and Planetary Science Letters*, *89*, 353-362

770 Schlosser, P., M. Stute, C. Sonntag, and K. O. Muennich (1989), Tritiogenic 3 He in
771 shallow groundwater, *Earth and Planetary Science Letters*, *94*, 245-256

772 Sorey, M. L., W. C. Evans, B. M. Kennedy, C. D. Farrar, L. J. Hainsworth, and B.
773 Hausback (1998), Carbon dioxide and helium emissions from a reservoir of
774 magmatic gas beneath Mammoth Mountain, California (Paper 98JB01389), *Journal*
775 *of Geophysical Research-Part B-Solid Earth*, *103*, 15303-15324

776 St-Jean, G. (2003), Automated quantitative and isotopic (C-13) analysis of dissolved
777 inorganic carbon and dissolved organic carbon in continuous-flow using a total
778 organic carbon analyser, *Rapid Communications in Mass Spectrometry*, *17*, 419-428

779 Stute, M., and P. Schlosser (1999), Atmospheric noble gases, in *Environmental*
780 *Tracers in Subsurface Hydrology*, edited by P. G. Cook and A. L. Herczeg, pp. 349-377,
781 Kluwer Academic, Boston, MA

782 Torgersen, T., and W. B. Clarke (1985), Helium accumulation in groundwater, I: An
783 evaluation of sources and the continental flux of crustal 4 He in the Great Artesian
784 Basin, Australia, *Geochimica et Cosmochimica Acta*, *49*

785 Van der Hoven, S. J., and J. E. Moran (in review), A Reevaluation of Crustal
786 Radiogenic Helium Isotopic Ratios in Shallow Groundwater Systems, *Geochimica et*
787 *Cosmochimica Acta*

788 Van der Hoven, S. J., R. E. Wright, D. A. Carstens, and K. C. Hackley (2005), Radiogenic
789 helium 4 as a conservative tracer in buried-valley aquifers, *Water Resourses*
790 *Research*, *41*

791 West-Yost&Associates (2005), Groundwater Management Support Activities,
792 Groundwater Characterization Report

793

794

Figures

A.

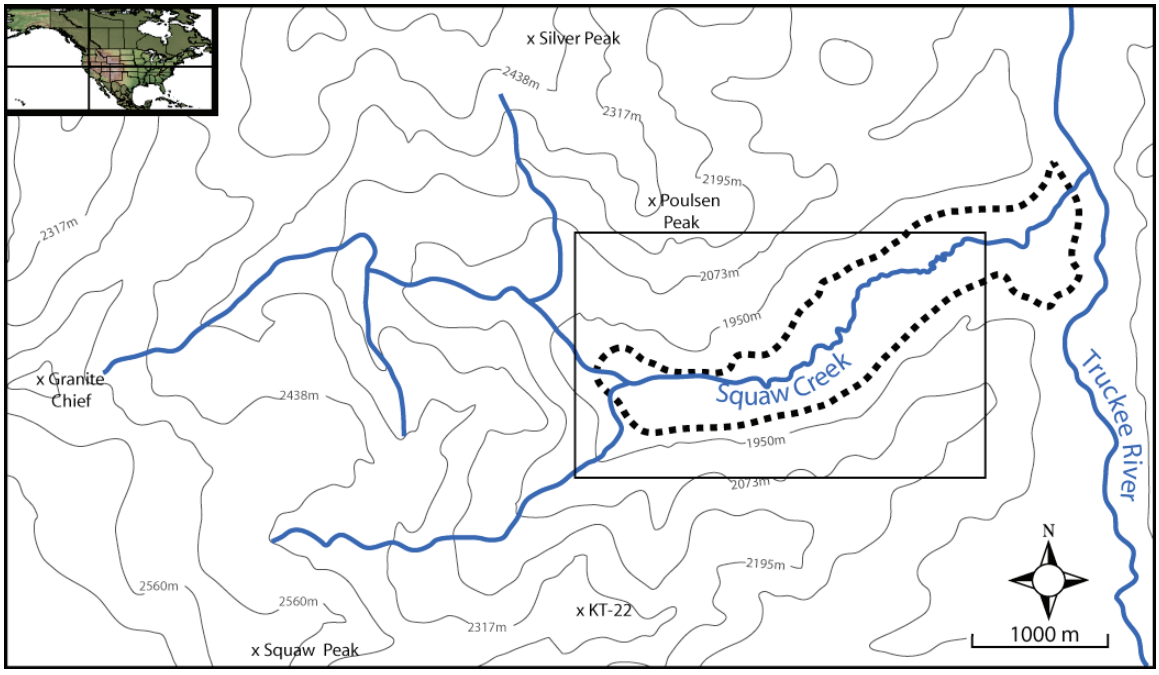

B.

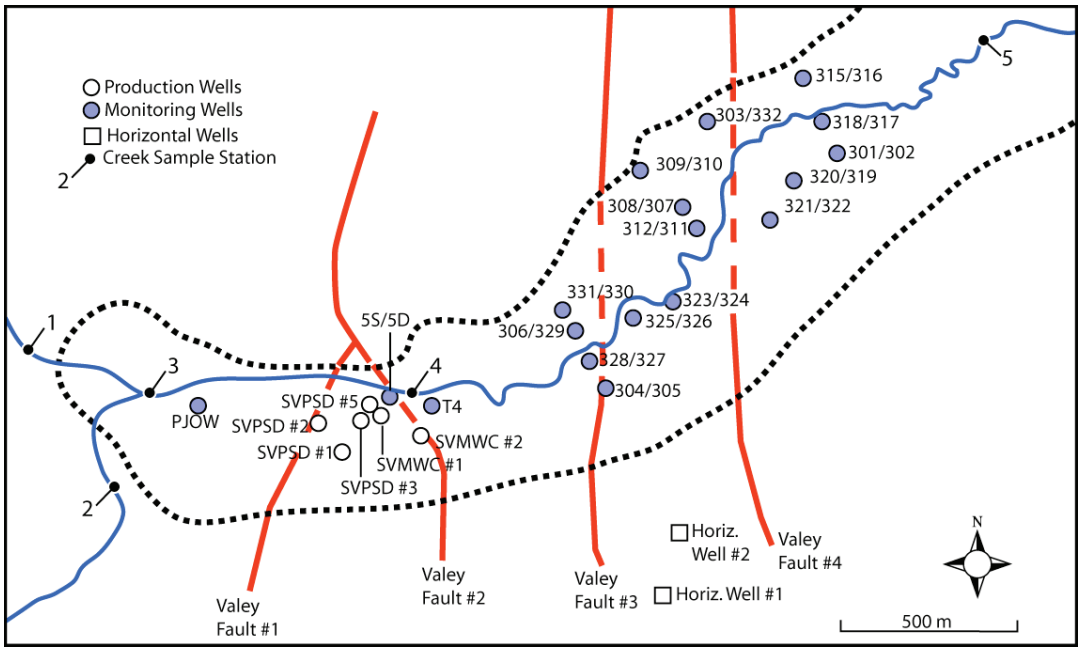

Figure 1. Topographic map (A) of the study area, and (B) locations of the wells and faults discussed in the text. The outline of the alluvial aquifer is shown as a dotted line after [*Hydrometrics-LLC*, 2007]. Stream sampling sites as labeled in Table 2 are 1) Shirley Canyon, 2)South Fork, 3)Confluence, 4)Trapezoid, and 5)Squaw Creek Rd Bridge.

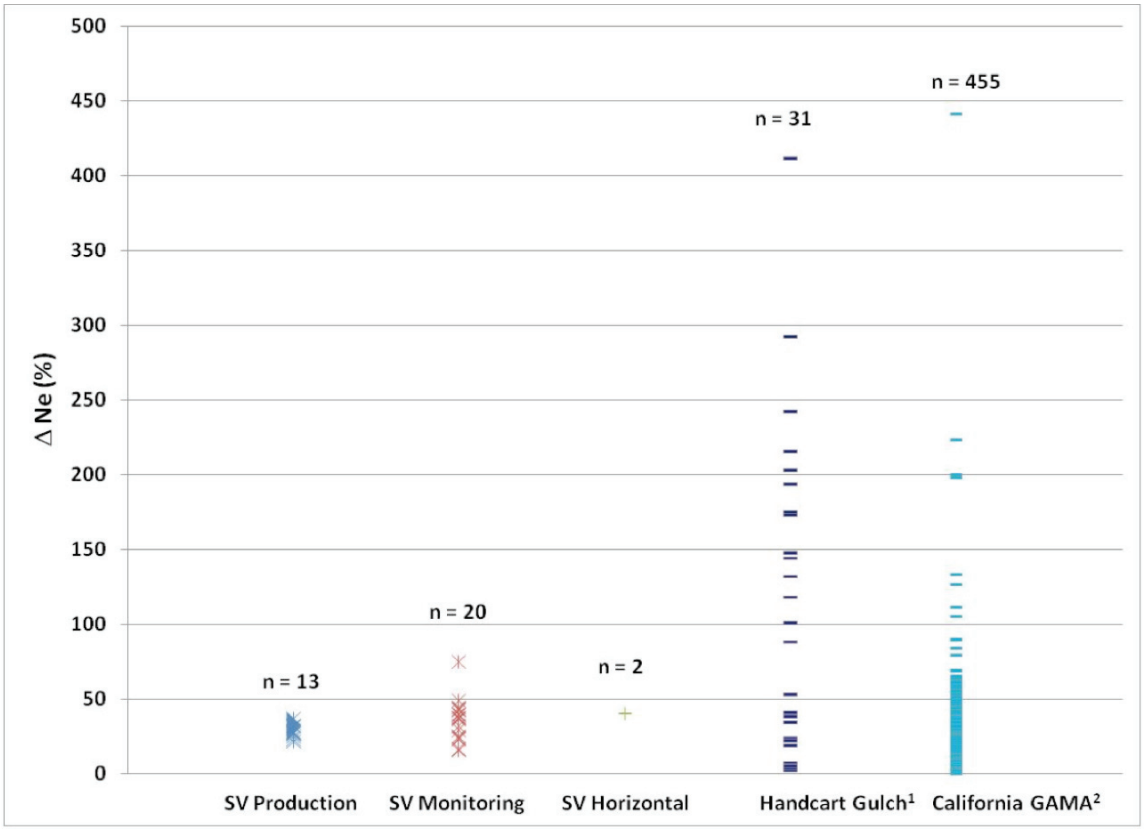

Figure 2. Observed ranges in excess air, expressed as ΔNe, for samples from Olympic Valley (categorized by well type), samples from the alpine watershed Handcart Gulch, and a large number of samples from around California sampled under the GAMA program.

[1] [*Manning and Caine*, 2007]

[2] [*Cey, et al.*, 2008]

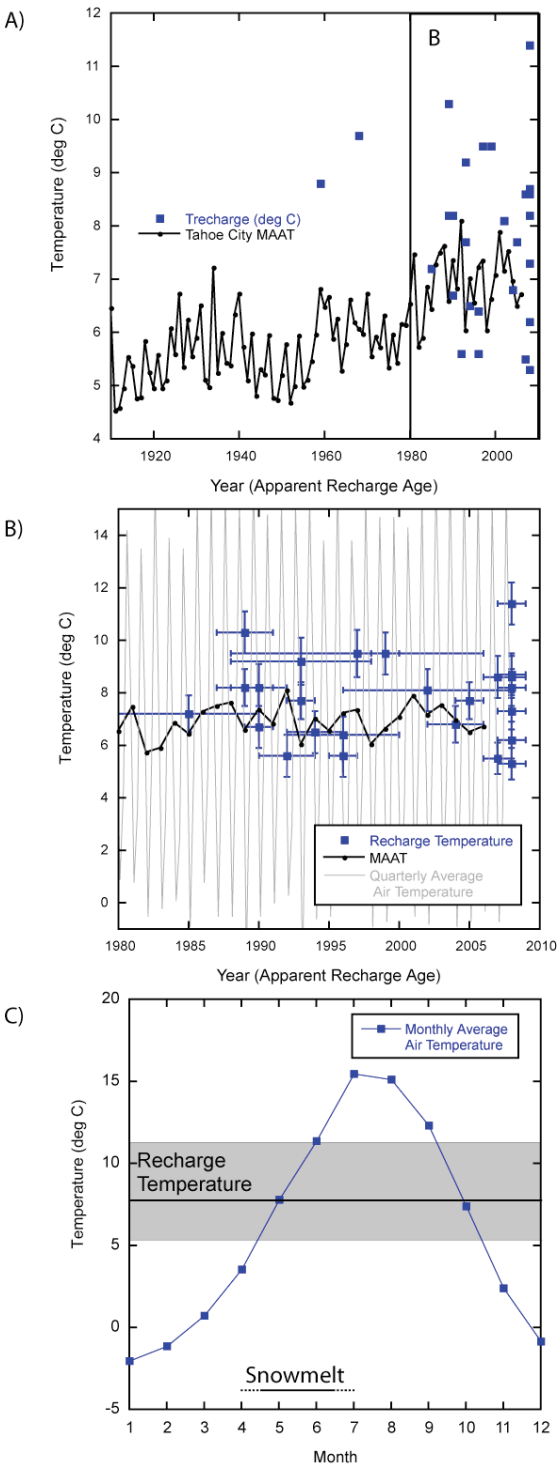

Figure 3. Noble gas recharge temperatures and apparent groundwater ages shown with mean annual air temperature (A, B), quarterly air temperature (B), and average monthly air temperature (C) at the NASA/GISS station at Tahoe City, CA. The range (shaded) and average (horizontal line) of recharge temperatures, along with the typical snowmelt season are shown on C.

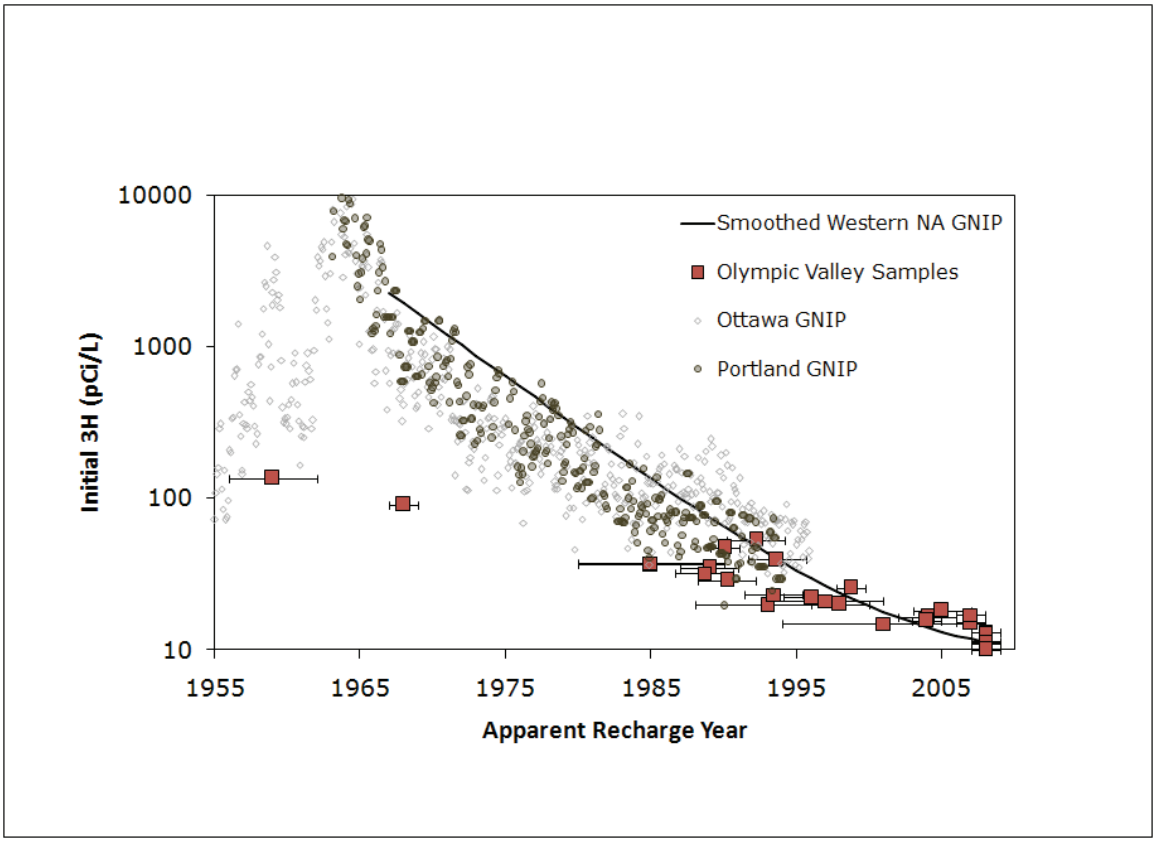

Figure 4. Tritium concentrations measured in precipitation at two locations where long IAEA GNIP records exist, along with an exponential curve that approximates mean annual values from western North America. Results for Olympic Valley well samples are plotted according to the calculated apparent tritium helium age (recharge year) and the measured tritium + tritiogenic ^{3}He (initial ^{3}H). Points that fall well below the curve contain a significant component of pre-modern water.

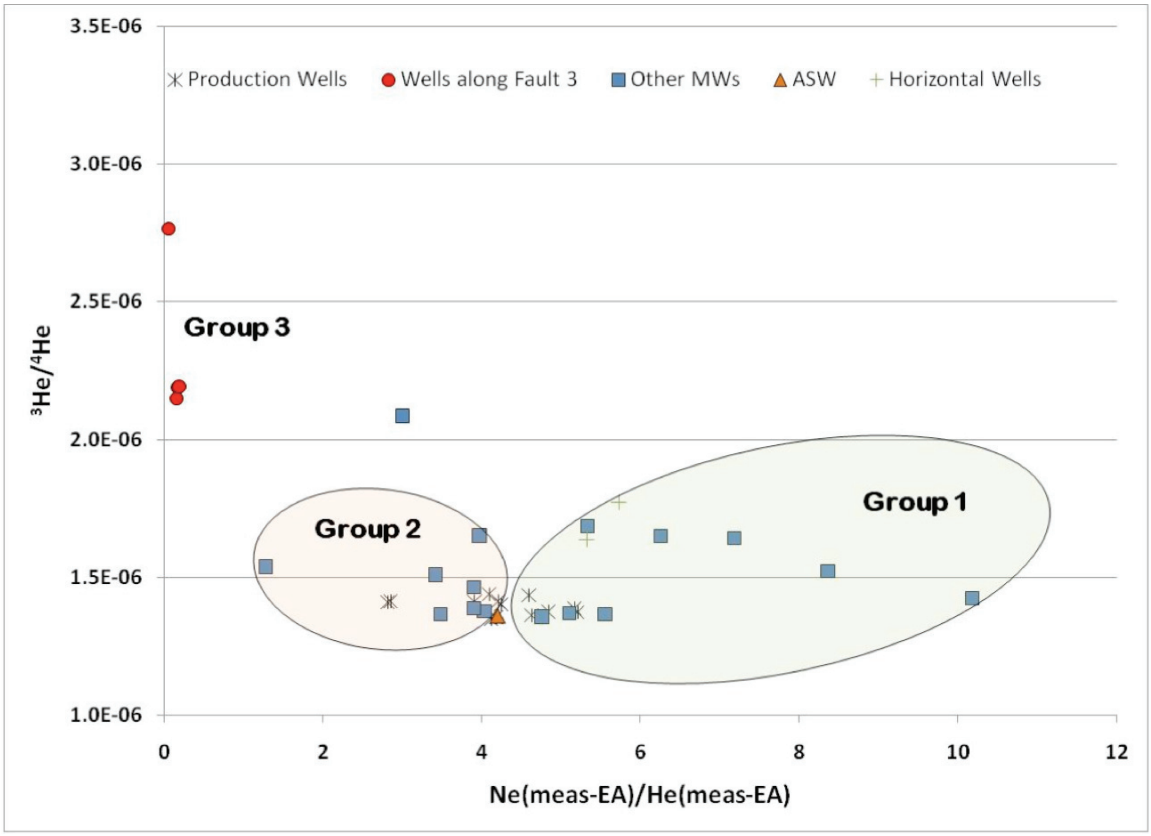

Figure 5. A plot of the ratio of Ne/He (measured concentration minus amount due to excess air) versus the measured $^{3}He/^{4}He$ ratio. Samples in Group 1 with very young ages are close to solubility values; significant amounts of tritiogenic ^{3}He bring some samples above the solubility ratio of $1.364x10^{-6}$. Group 2 samples are affected by crustal He, which results in a decrease in Ne/He and by tritiogenic ^{3}He. Group 3 samples are affected by magmatic He. Orange triangle represents air saturated water at 8ºC.

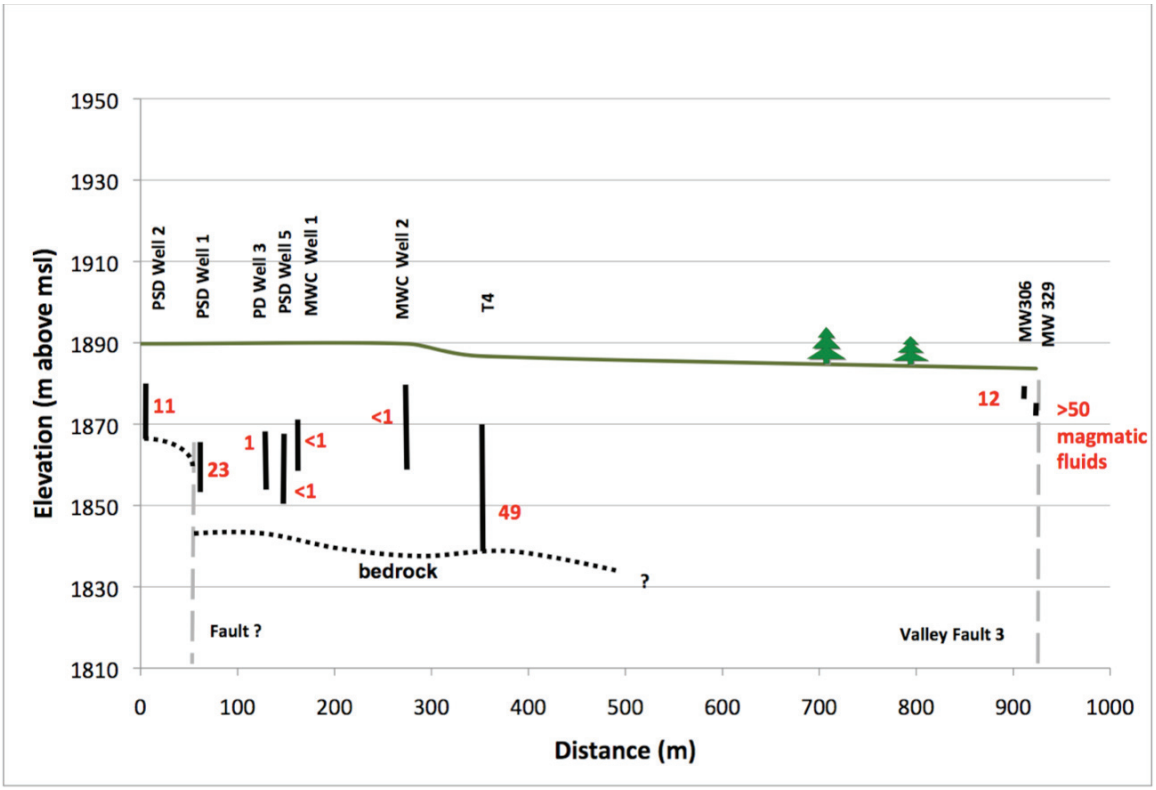

Figure 6. Schematic cross section through Olympic Valley running along Squaw Creek, showing the approximate locations of the major faults and the depth to bedrock as based on well logs [*West-Yost&Associates*, 2005] by seismic profiling [*Gasch&Associates*, 1973]. Solid vertical lines represent screened intervals for wells on or close to the cross section, with labels indicating the mean apparent tritium-helium groundwater age. Vertical exaggeration is 10X.

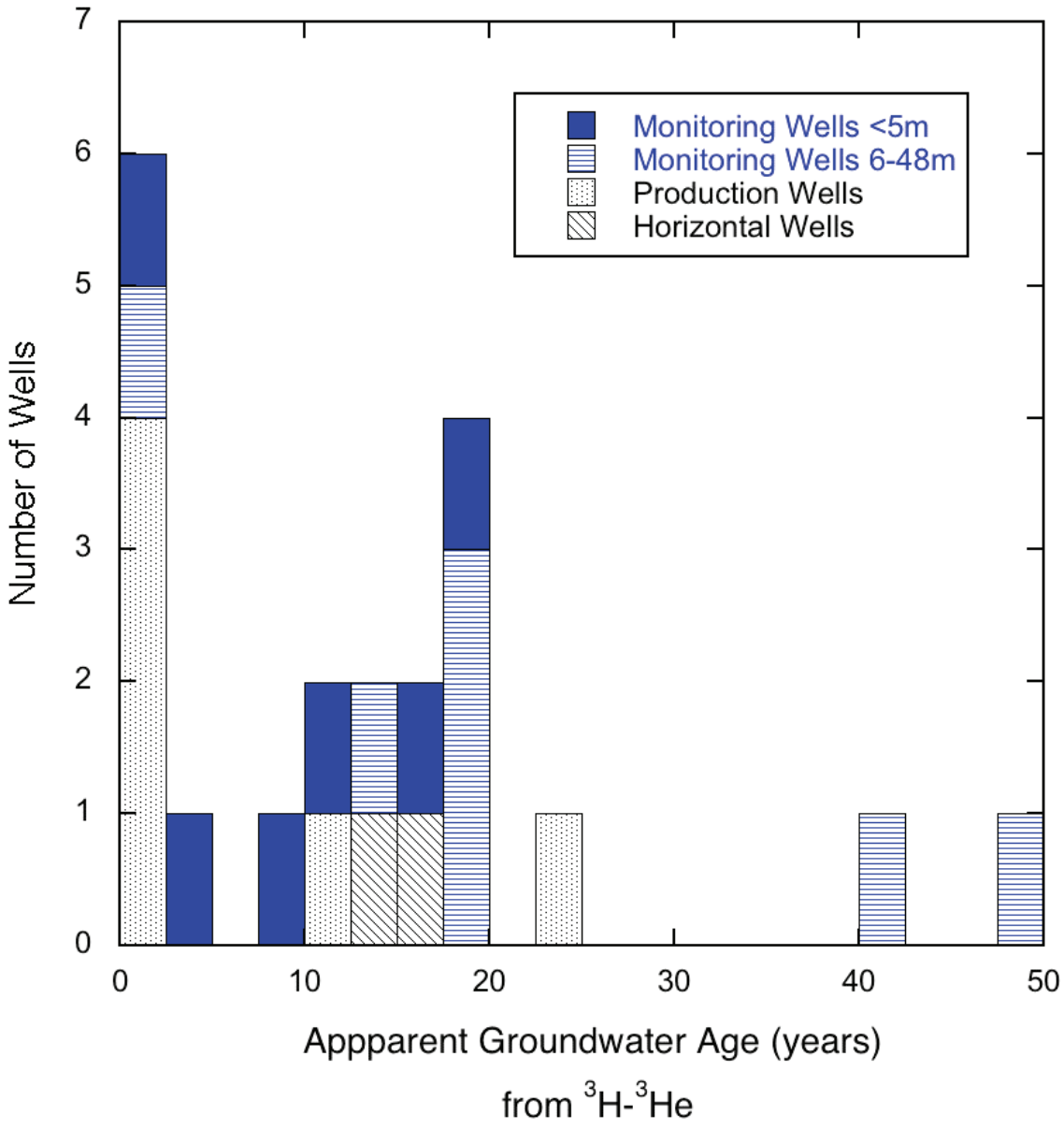

Figure 7. Histogram of apparent groundwater ages. Average apparent ages are plotted for wells that were sampled more than once.

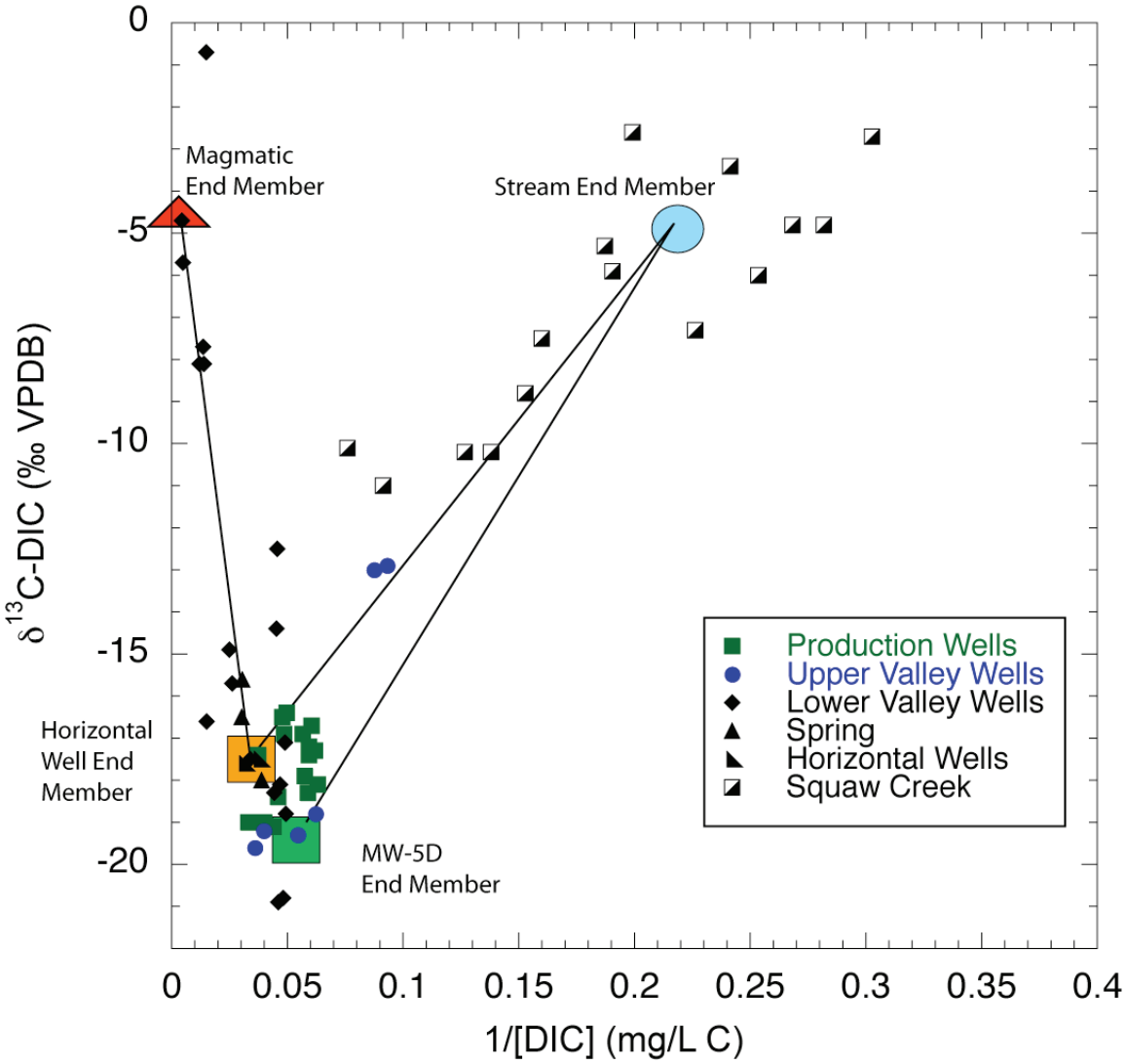

Figure 8. Stable carbon isotope compositions (δ^{13}C-DIC) and inverse concentration of dissolved inorganic carbon for wells, a spring, and creek water in the Olympic Valley study area. Mixing lines are plotted between two potential end members for groundwater recharge through soils, a magmatic water end member, and a stream end member.

Table 1. Measurements of dissolved gas and isotopic compositions from horizontal wells “HW”, monitoring wells “MW”, production wells “PW”, a spring “SP”, and stream waters “SW”.

Sample Site	Collection Date	Sample Type	Screen depth (m)	DIC (mg/L C)	$\delta^{13}C$ (‰ VPDB)	^{3}H (pCi/L)	+/-	$^{3}He/^{4}He$	+/-	^{4}He (cc STP/g)	+/-	Ar (cc STP/g)	+/-	Kr (cc STP/g)	+/-	Ne (cc STP/g)	+/-	Xe (cc STP/g)	+/-
Horizontal Well 1	06/19/2008	HW		26	-17.5	17.6	1.1	1.64E-06	5.09E-08	6.49E-08	2.07E-09	4.00E-04	7.99E-06	8.99E-08	2.70E-09	2.83E-07	5.67E-09	1.25E-08	3.75E-10
Horizontal Well 2	06/19/2008	HW		32	-17.6	21.8	1.2	1.77E-06	5.52E-08	6.07E-08	1.94E-09	4.15E-04	8.30E-06	9.22E-08	2.77E-09	2.76E-07	5.53E-09	1.28E-08	3.85E-10
MW 301	05/13/2008	MW	3-5	38	-15.7	10.2	0.9	1.65E-06	1.24E-08	3.56E-08	7.12E-10	3.42E-04	6.84E-06	7.75E-08	2.32E-09	1.98E-07	3.96E-09	1.15E-08	3.45E-10
MW 302	05/13/2008	MW	12-14	40	-14.9	9.8	0.9	2.09E-06	1.56E-08	6.79E-08	1.36E-09	3.39E-04	6.78E-06	7.66E-08	2.30E-09	2.11E-07	4.22E-09	1.08E-08	3.25E-10
MW 303	06/18/2008	MW	3-5	20	-18.8	11.5	1.4	1.46E-06	4.25E-08	6.67E-08	1.33E-09	3.53E-04	7.07E-06	7.78E-08	2.33E-09	2.49E-07	4.99E-09	1.12E-08	3.36E-10
MW 304	05/14/2008	MW	3-5	73	-7.7	6.3	0.6	2.19E-06	1.64E-08	9.53E-07	1.91E-08	3.85E-04	7.70E-06	8.39E-08	2.52E-09	2.80E-07	5.60E-09	1.24E-08	3.72E-10
MW 305	05/14/2008	MW	11-13	72	-8.1	6.4	0.6	2.15E-06	1.61E-08	1.02E-06	2.04E-08	3.87E-04	7.73E-06	8.53E-08	2.56E-09	2.64E-07	5.28E-09	1.20E-08	3.60E-10
MW 306	05/14/2008	MW	2-3	21	-20.8	11.4	1.4	1.52E-06	1.14E-08	5.74E-08	1.15E-09	4.11E-04	8.21E-06	9.09E-08	2.73E-09	2.99E-07	5.97E-09	1.31E-08	3.93E-10
MW 309	06/18/2008	MW	3-5	22	-14.4	17.8	1.5												
MW 310	06/18/2008	MW	11-12	22	-20.9	10.6	1.4	1.64E-06	4.77E-08	5.30E-08	1.06E-09	3.75E-04	7.50E-06	8.19E-08	2.46E-09	2.67E-07	5.33E-09	1.18E-08	3.55E-10
MW 315	06/18/2008	MW	2-3	77	4.2	11.3	1.0												
MW 316	06/18/2008	MW	8-10	66	-16.6	10.4	1.4												
MW 318	05/13/2008	MW	3-5	67	-0.7	16.9	1.1												
MW 321	05/14/2008	MW	3-5	29	-17.5	10.8	1.4	1.68E-06	1.26E-08	5.28E-08	1.06E-09	3.33E-04	6.67E-06	7.61E-08	2.28E-09	2.41E-07	4.81E-09	1.08E-08	3.25E-10
MW 322	05/14/2008	MW	17-18	21	-18.1	14.6	1.5	1.65E-06	1.24E-08	7.06E-08	1.41E-09	3.82E-04	7.64E-06	8.58E-08	2.57E-09	2.66E-07	5.33E-09	1.24E-08	3.72E-10
MW 327	05/14/2008	MW	11-13	83	-8.1														
MW 328	05/14/2008	MW	3-5	23	-18.3	12.4	1.4	1.42E-06	1.07E-08	5.37E-08	1.07E-09	3.68E-04	7.35E-06	8.67E-08	2.60E-09	2.96E-07	5.91E-09	1.25E-08	3.76E-10
MW 329	05/14/2008	MW	13-15	203	-5.7	0.3	0.7	2.77E-06	3.40E-08	2.91E-06	5.82E-08	4.26E-04	8.52E-06	8.95E-08	2.69E-09	3.17E-07	6.34E-09	1.32E-08	3.95E-10
MW 330	05/13/2008	MW	8-9	222	-4.7	-0.5	0.9												
MW 331	05/13/2008	MW	2-3	20	-17.1	12.0	1.0	1.51E-06	1.13E-08	6.19E-08	1.24E-09	3.50E-04	7.00E-06	8.02E-08	2.41E-09	2.13E-07	4.26E-09	1.14E-08	3.42E-10
MW 5D	05/13/2008	MW	12-14	18	-19.3	8.7	0.6	1.36E-06	1.02E-08	7.38E-08	1.48E-09	3.63E-04	7.26E-06	7.95E-08	2.38E-09	2.58E-07	5.15E-09	1.14E-08	3.41E-10
MW 5D	08/12/2008	MW	12-14	16	-18.8	9.1	1.0	1.39E-06	8.05E-08	6.74E-08	5.50E-09	3.53E-04	7.05E-06	8.03E-08	2.41E-09	2.52E-07	5.03E-09	1.12E-08	3.37E-10
MW 5S	05/13/2008	MW	6-8	28	-19.6	11.4	0.7	1.37E-06	1.02E-08	4.84E-08	9.69E-10	3.81E-04	7.63E-06	8.58E-08	2.57E-09	2.29E-07	4.58E-09	1.16E-08	3.47E-10
MW 5S	08/12/2008	MW	6-8	25	-19.2	11.7	1.0	1.37E-06	7.94E-08	4.54E-08	3.70E-09	3.20E-04	6.40E-06	7.39E-08	2.22E-09	2.08E-07	4.15E-09	1.03E-08	3.08E-10
MW PJOW	05/13/2008	MW	24-26	11	-13.0	10.3	1.0	1.38E-06	1.03E-08	4.74E-08	9.49E-10	3.43E-04	6.87E-06	8.47E-08	2.54E-09	1.87E-07	3.73E-09	1.24E-08	3.71E-10
MW PJOW	08/12/2008	MW	24-26	11	-12.9	9.3	0.9	1.36E-06	7.87E-08	4.59E-08	3.75E-09	3.48E-04	6.97E-06	8.65E-08	2.59E-09	2.01E-07	4.02E-09	1.26E-08	3.78E-10
MW T4	09/26/2008	MW	16-48	22	-12.5	8.7	0.6	1.54E-06	2.09E-08	1.57E-07	3.13E-09	3.72E-04	7.45E-06	8.36E-08	2.51E-09	2.64E-07	5.27E-09	1.15E-08	4.04E-10
MWC Well 1	04/25/2008	PW	18-30	22	-18.4	10.0	0.4	1.37E-06	1.03E-08	NM		3.69E-04	7.39E-06	8.22E-08	2.47E-09	2.48E-07	4.97E-09	1.14E-08	3.42E-10
MWC Well 1	08/12/2008	PW	18-30	23	-19.1	11.1	0.9	1.43E-06	8.32E-08	5.67E-08	4.63E-09	3.57E-04	7.15E-06	8.12E-08	2.44E-09	2.37E-07	4.74E-09	1.16E-08	3.49E-10
MWC Well 2	04/25/2008	PW	11-30	30	-19.0	10.1	0.4	1.36E-06	1.02E-08	NM		3.83E-04	7.67E-06	8.22E-08	2.47E-09	2.31E-07	4.61E-09	1.23E-08	3.69E-10
MWC Well 2	08/12/2008	PW	11-30	25	-19.0	11.6	1.0	1.37E-06	4.27E-08	5.34E-08	1.71E-09	3.64E-04	7.28E-06	8.30E-08	2.49E-09	2.41E-07	4.81E-09	1.14E-08	3.42E-10
SVPSD Well1	04/25/2008	PW	23-34	21	-16.9	9.6	0.4												
SVPSD Well1	06/18/2008	PW	23-34	21	-16.5	10.2	2.7	1.41E-06	4.10E-08	7.50E-08	1.50E-09	3.64E-04	7.29E-06	8.29E-08	2.49E-09	2.25E-07	4.50E-09	1.19E-08	3.58E-10
SVPSD Well1	08/12/2008	PW	23-34	20	-16.4			1.41E-06	8.18E-08	7.99E-08	6.52E-09	3.75E-04	7.50E-06	8.96E-08	2.69E-09	2.40E-07	4.80E-09	1.24E-08	3.73E-10
SVPSD Well2	04/25/2008	PW	10-23	17	-17.2	11.3	0.5												
SVPSD Well2	06/18/2008	PW	10-23	17	-16.7	10.0	1.0	1.44E-06	4.17E-08	5.77E-08	1.15E-09	3.65E-04	7.31E-06	8.49E-08	2.55E-09	2.26E-07	4.52E-09	1.23E-08	3.68E-10
SVPSD Well2	08/12/2008	PW	10-23	16	-18.1			1.41E-06	8.18E-08	5.56E-08	4.54E-09	3.50E-04	7.01E-06	8.49E-08	2.55E-09	2.12E-07	4.23E-09	1.19E-08	3.57E-10
SVPSD Well3	04/25/2008	PW	22-35	17	-17.4	10.4	0.4	1.35E-06	1.01E-08	NM		3.65E-04	7.29E-06	7.95E-08	2.39E-09	2.15E-07	4.29E-09	1.18E-08	3.54E-10
SVPSD Well3	06/18/2008	PW	22-35	18	-16.9	10.5	1.0	1.41E-06	4.10E-08	5.43E-08	1.09E-09	3.56E-04	7.13E-06	8.29E-08	2.49E-09	2.18E-07	4.35E-09	1.20E-08	3.61E-10
SVPSD Well5	04/25/2008	PW	22-39	17	-18.3	10.3	0.4	1.36E-06	1.02E-08	5.75E-08	1.15E-09	3.63E-04	7.26E-06	7.97E-08	2.39E-09	2.28E-07	4.56E-09	1.19E-08	3.56E-10
SVPSD Well5	06/18/2008	PW	22-39	17	-17.9	16.1	2.7	1.39E-06	4.03E-08	5.88E-08	1.18E-09	3.74E-04	7.49E-06	8.21E-08	2.46E-09	2.58E-07	5.16E-09	1.16E-08	3.47E-10
SVPSD Well5	08/12/2008	PW	22-39	16	-17.3	12.8	1.0	1.40E-06	4.37E-08	5.49E-08	1.76E-09	3.49E-04	6.98E-06	7.99E-08	2.40E-09	2.20E-07	4.41E-09	1.17E-08	3.51E-10
Upwelling	04/25/2008	SP		33	-16.5														
Upwelling	05/14/2008	SP		33	-15.6	10.7	0.9												
Upwelling	08/12/2008	SP		26	-18.0														
Confluence	04/25/2008	SW		7	-10.2	10.5	0.4												
Confluence	05/14/2008	SW		4	-4.8														
Confluence	06/19/2008	SW		4	-3.4														
Shirley Canyon	04/25/2008	SW		5	-5.3	10.5	0.5												
Shirley Canyon	05/14/2008	SW		4	-4.8														
Shirley Canyon	06/18/2008	SW		3	-2.7														
South Fork at Bridge	04/25/2008	SW		6	-7.5	12.4	0.5												
South Fork at Bridge	05/14/2008	SW		4	-6.0														
South Fork at Bridge	06/18/2008	SW		5	-2.6														
Squaw Creek Rd bridge	04/25/2008	SW		8	-10.2	11.5	0.5												
Squaw Creek Rd bridge	05/14/2008	SW		4	-7.3														
Squaw Creek Rd bridge	06/19/2008	SW		5	-5.9														
Squaw Creek Rd bridge	08/12/2008	SW		11	-11.0														
Squaw Creek Rd bridge	09/25/2008	SW		13	-10.1	9.7	0.5												
Trapezoid	04/25/2008	SW		7	-8.8	12.0	0.5												

NM = Measurement failed

Table 2. Calculations based on noble gas concentrations and isotope ratios.

Well Name	Date	Screen depth (m)	ΔNe	$^4He_{rad}$	+/-	$T_{recharge}$ (deg C)[1]	+/-	χ^2	Age[2]	+/-	% Pre-modern
Upper Valley MW's											
MW PJOW	5/13/08	24-26	17%	4.46E-09	1.63E-09	5.5	0.6	1.0	1	1	<10%
MW PJOW	8/12/08	24-26	24%	<2.0E-09		5.3	0.6	3.1	<1	1	<10%
MW 5D	5/13/08	12-14	38%	1.18E-08	4.12E-09	9.2	0.9	0.3	15	5	52%
MW 5D	8/12/08	12-14	37%	6.32E-09	3.84E-09	9.5	0.9	0.8	11	9	40%
MW 5S	5/13/08	6-8	30%	<2.0E-09		8.2	0.7	11.0	<1	1	<10%
MW 5S	8/12/08	6-8	25%	<2.0E-09		11.4	0.8	0.5	<1	1	<10%
MW T4	9/26/08	16-48	37%	9.40E-08	4.79E-09	8.8	0.9	0.4	49	3	98%
Production wells											
SVPSD Well1	6/18/08	23-34	27%	2.23E-08	2.81E-09	7.2	0.7	0.4	23	5	72%
SVPSD Well1	8/12/08	23-34	31%	2.32E-08	3.43E-09	6.2	0.7	1.2			
SVPSD Well2	6/18/08	10-23	27%	4.76E-09	2.81E-09	6.4	0.7	0.0	12	4	21%
SVPSD Well2	8/12/08	10-23	23%	5.78E-09	2.27E-09	7.1	0.7	1.3			
SVPSD Well3	4/25/08	22-35	23%	4.09E-09	2.36E-09	7.3	0.7	3.0	<1	1	<10%
SVPSD Well3	6/18/08	22-35	25%	NM		6.8	0.7	0.1	4	2	<10%
SVPSD Well5	4/25/08	22-39	28%	3.82E-09	2.90E-09	7.3	0.7	1.3	<1	1	<10%
SVPSD Well5	6/18/08	22-39	37%	*<2.0E-09*		8.6	0.8	0.5	1	1	<10%
SVPSD Well5	8/12/08	22-39	27%	*2.66E-09*	2.63E-09	7.7	0.7	0.8	3	1	<10%
MWC Well 1	4/25/08	18-30	27%	*<2.0E-09*		8.6	0.8	4.1	<1	1	<10%
MWC Well 1	8/12/08	18-30	32%	*<2.0E-09*		8.1	0.8	0.2	6	6	<10%
MWC Well 2	4/25/08	11-30	22%	*<2.0E-09*		6.2	0.7	7.5	<1	1	<10%
MWC Well 2	8/12/08	11-30	31%	*<2.0E-09*		8.7	0.8	1.4	<1	1	<10%
Horizontal Wells											
Horizontal Well 1	6/19/08		41%	*<2.0E-09*		6.5	0.8	0.6	14	2	<10%
Horizontal Well 2	6/19/08		40%	*<2.0E-09*		5.6	0.8	3.5	16	2	<10%
Lower Valley MW's											
Shallow (2-5 m BGS)											
MW 301	5/13/08	3-5	16%	<2.0E-09		7.7	0.7	0.7	15	1	43%
MW 303	6/18/08	3-5	37%	6.21E-09	3.75E-09	9.5	0.8	1.0	9	1	34%
MW 304	5/14/08	3-5	43%	8.85E-07	1.84E-08	7.0	0.9	2.0	^{3}He excess		NA
MW 306	5/14/08	2-3	43%	<2.0E-09		5.6	0.8	0.1	12	1	25%
MW 321	5/14/08	3-5	32%	<2.0E-09		10.3	0.8	2.6	19	2	59%
MW 328	5/14/08	3-5	44%	<2.0E-09					4	1	<10%
MW 331	5/13/08	2-3	24%	1.18E-08	2.33E-09	8.2	0.7	0.4	19	2	54%
Deep (11-18 m BGS)											
MW 302	5/13/08	12-14	24%	1.80E-08	2.29E-09	9.7	0.7	0.4	40	1	95%
MW 305	5/14/08	11-13	39%	9.54E-07	1.96E-08	7.7	0.8	0.4	^{3}He excess		NA
MW 310	6/18/08	11-12	40%	<2.0E-09		8.2	0.9	0.5	18	2	54%
MW 322	5/14/08	17-18	38%	7.27E-09	4.53E-09	6.7	0.8	0.3	18	1	52%
MW 327	5/14/08	11-13	75%	8.03E-07	2.53E-08	9.2	2.5	0.1	^{3}He excess		NA
MW 329	5/14/08	13-15	49%	2.83E-06	5.70E-08	5.9	0.9	0.8	^{3}He excess		NA

1 An elevation of 1950 m used to determine pressure, except at the two horizontal wells, where an elevation of 2050 m is applied.

2 A crustal $^3He/^4He$ ratio of $6x10^{-7}$ is used in the age determination for samples with $[He_{meas} - (He_{sol} + He_{xs\ air})] > 2x10^{-9}$.